Spin Flipper and Neutron Polarimetry for the n^{3}He Experiment

C. B. Hayes

November 13, 2014

Abstract

The Spallation Neutron Source (SNS) at Oak Ridge National Laboratory is a pulsed source of neutrons generated by a 1 GeV proton beam colliding with a liquid Mercury target at 60 Hz. The n^{3}He experiment, constructed on Fundamental neutron Physics Beamline-13 (FnPB-13), is designed to measure the parity violating (PV) proton asymmetry A_p in the nuclear reaction

$$n + {}^3_2\mathrm{He} = {}^3_1\mathrm{H} + {}^1_1\mathrm{H} + 765\,\mathrm{KeV} \tag{0.1}$$

The asymmetry is directly related to the weak isospin conserved couplings h^0_ρ and ω^0_ρ which are of fundamental interest in the verification of the meson exchange model of low energy NN intereactions. Theoretical estimates suggest a value of $A_p \sim 3 \times 10^{-7}$. The statistical uncertainty in the measurement of A_p is governed by

$$\delta A_p = \left[\frac{\sigma_d}{P\sqrt{N}}\right] \tag{0.2}$$

where $\sigma_d(\approx 6)$ is the intrinsic detector effeciency, $P(\approx 96\%)$ is the beam polarization, and N is the total number of neutrons involved in the experiment. With a flux of neutrons on the order of 2×10^{11} per second, the experiment will have a statistical sensitivity of $\delta A_p \sim 2 \times 10^{-8}$ in an estimated 116 days of run time.

In real time, the experiment will probably last about one year. Of high importance will be several polarimetry measurements to monitor beam polarization and spin flipper efficiency during production of data and also after completion of the experiment. Polarimetry will also be required before data production for initial calibration and tests of the spin flipper.

1 Theory of the Hadronic Weak Interaction

The theory of the weak interaction is mediated by the short range $W^{\pm}$ and Z^0 vector bosons. It is a well understood theory by itself, but cannot be applied directly in a reaction like equation (0.1) which is overwhelming dominated by strong QCD effects. Instead, it becomes necessary to develop a theory of the Weak Hadronic Interaction (HWI) which takes into account both strong and weak couplings simultaneously.

The first successful theory of the HWI, called the *Meson Exchange Model*, was introduced by Desplanques, Donoghue, and Holstein [1] in 1980. In this model, the strong interaction between hadrons is mediated by light virtual mesons π, ρ, and ω. Figure 1 shows how a small weak component to the interaction is introduced by allowing the mediator to decay weakly before coupling to the second vertex. While

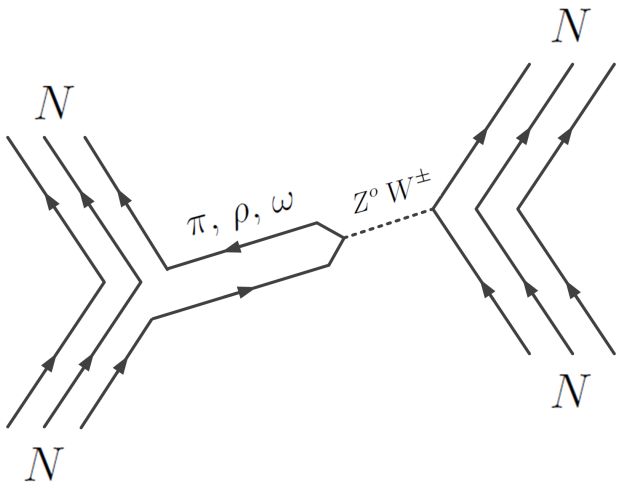

Figure 1: The range of $W^{\pm}$ and Z^0 bosons is to short for a direct interaction between nucleons. Instead, the interaction is possible thru the decay of π, ρ, and ω.

the weak component represented by this diagram is 10^{-7} times smaller than its strong counterpart, it is detectable experimentally as a result of the parity violation (PV) property of the weak force.

In general, obsevables in the Meson Exchange Model are constructed from 6 unknown coupling contants which must be measured experimentally. The most general equation for an observable A can be written

$$A = a_{\pi}^{1} \cdot h_{\pi}^{1} + a_{\rho}^{0} \cdot h_{\rho}^{0} + a_{\rho}^{1} \cdot h_{\rho}^{1} + a_{\rho}^{2} \cdot h_{\rho}^{2} + a_{\omega}^{0} \cdot h_{\omega}^{0} + a_{\omega}^{1} \cdot h_{\omega}^{1} \tag{1.1}$$

where the superscript indicates the isospin carried by the particle. The observable for the n^{3}He experiment is the PV asymmetry A_p of the outgoing proton. All terms in (1.1) conribute to the interaction but only three of them are significant. An approximation of A_p simplifies the general expression to

$$A_p = -0.18 \cdot h_{\pi}^{1} - 0.14 \cdot h_{\rho}^{0} - 0.13 \cdot h_{\omega}^{0} \tag{1.2}$$

The coupling constant h_π^1 has been measured to an accuracy of less hn 5% by the recently completed NPDGamma experiment. The overall goal of n^{3}He is therefore an assessment of the zero isospin couplings h_ρ^0, and h_ω^0 of the Meson Exchange Model. Feynman diagrams associated with all couplings in (1.2) are indicated by figures 2 and 3 for reference.

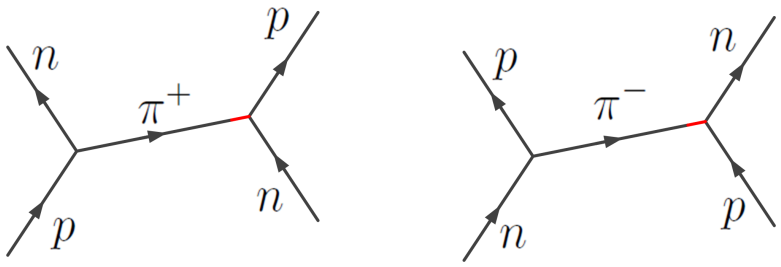

Figure 2: The strong vertex on the left side of each diagram is associated with the meson coupling constant h_π^1. The exchange of a π^o is not possible here since neutral spinless mesons do not contribute to parity violation.

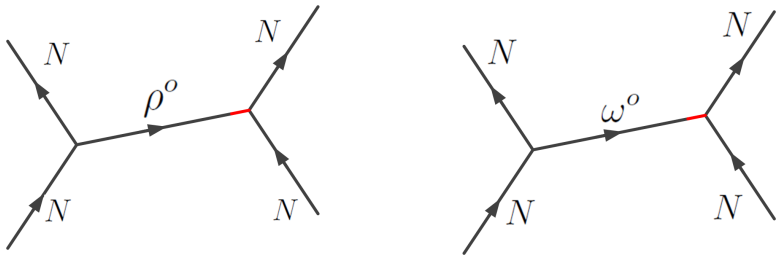

Figure 3: The ρ^o and ω^o are both vector particles. They carry no isospin and no charge so both nucleons N connected to each vertex are the same.

2 Details of the n^{3}He Experiment

The design of the n^{3}He experiment is illustrated in figure 4. Pulses of neutrons emerging from a super mirror polarizer (SMP) are spin aligned transverse to the direction of motion. Individual pulses enter the RFSR which is synchronized to the arrival of each pulse and becomes energized to flip the spins of alternating pulses with an efficiency approaching 100 percent. Neutrons emerging from the RFSR interact with ^{3}He in the ion chamber producing protons and tritium in accordance with (0.1). The value of A_p can be extracted from measurements of electrical currents induced in wire planes within the ion chamber.

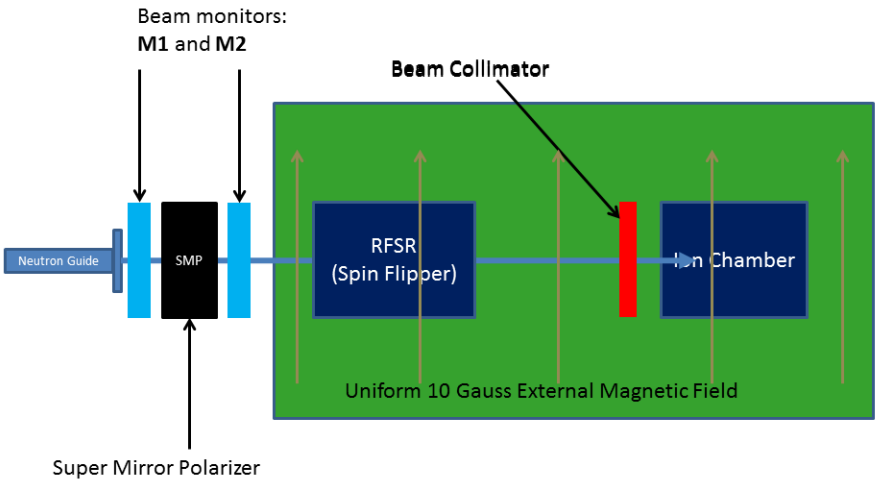

Figure 4: Design of the n^3He experiment. Complex data acquisition electronics attached to the ion chamber are not shown here.

The success of this measurment hinges on the successful elimination of false asymmetries to at least an order of magnitude less than δA_p which can be achieved thru a precision alignment of the ion chamber with the transverse holding field. Even with precise alignment however the success of the experiment relies on high efficiency operation of the RFSR and sound data acquisition electronics.

3 Spin Flipper

The spin flipper is a major component of the n^3He experiment. It is a new design based on the theory of double cosine theta coils, and is the first one of its kind. Two of the most impressive properties of the spin flipper are its highly uniform interior field, and its ability to flip either transverse or longitudinally polarized neutrons.

3.1 Design and Construction of the Spin Flipper

Pictures of the completed spin flipper are shown in figure 5. The interior of the device is composed two grooved outer return coils (having semi-circular cross-sections) which fit snugly around a grooved inner cylinder. The grooves are precisely machined to accomodate about 870 feet of 18 AWG solid aluminum wire. The intricate pattern of grooves is based on the theory of double cosine theta coils and serves the purpose of

producing a uniform transverse magnetic field in the region inside the inner cylinder.

The coils are enclosed by a 1/4 inch thick cylindrical aluminum shell and two 1/4 inch thick end plates with square insets machined to 40 mils. The end plates are sealed to the cylinder with RTV Silicon so that the device can filled with ^{4}He gas to prevent scattering of neutrons during use. The housing on top of the shell accomodates a parallel connection of capacitors with a total capacitance of $C = 17.7\,\mathrm{nF}$.

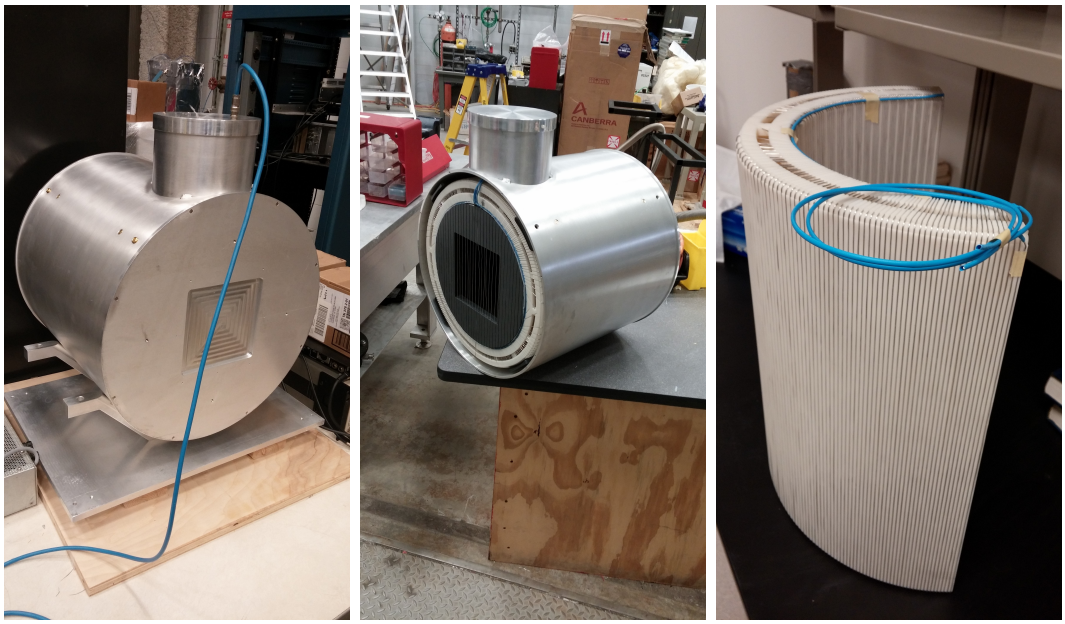

Figure 5: Pictures of the n^{3}He spin flipper. The inner cylinder is made from 12.5 inch PVC pipe and was machined by the UT machine shop. The outer return coils are ABS plastic and were extruded using an SLA (Stereolithographic) 3D print technology.

3.2 Fields of a Cos-Theta Coil

A ***cosine-theta coil*** is a long hollow cylindrical coil of radius R_{in} characterized by a spatially uniform magnetic field in its interior which is transverse to the symmetry axis of the coil. For the static problem, the cylinder can be characterized by an applied surface current density

$$\boldsymbol{k}(\phi) = k \sin\phi\, \hat{\boldsymbol{z}} \tag{3.1}$$

which is the continuum limit of a large number of wires. The resulting field is most easily determined using the theory of a magnetic scalar potential. In regions of zero current density the magnetic field is characterized by

$$\boldsymbol{\nabla} \times \boldsymbol{H} = 0 \tag{3.2}$$

which determines the scalar potential from the relation $\boldsymbol{H} = -\boldsymbol{\nabla} U$.

For reference, transformation equations for the unit vectors in cartesian and polar coordinates are:

$$\hat{\boldsymbol{r}} = \cos\phi\,\hat{\boldsymbol{x}} + \sin\phi\,\hat{\boldsymbol{y}} \qquad \hat{\boldsymbol{x}} = \cos\phi\,\hat{\boldsymbol{r}} - \sin\phi\,\hat{\boldsymbol{\phi}}$$
$$\hat{\boldsymbol{\phi}} = -\sin\phi\,\hat{\boldsymbol{x}} + \cos\phi\,\hat{\boldsymbol{y}} \qquad \hat{\boldsymbol{y}} = \sin\phi\,\hat{\boldsymbol{r}} + \cos\phi\,\hat{\boldsymbol{\phi}}$$

Potentials and fields associated with the coil can be divided into two regions: $r \leq R_{in}$ and $r > R_{in}$. Since $\boldsymbol{\nabla} \cdot \boldsymbol{H}$=0, the general form of the scalar potential in either region will be a solution to Laplace's equation $\boldsymbol{\nabla}^2 U = 0$ and is of the general form

$$U(r,\phi) = a_o + b_o \ln r + \sum_{k=0}^{\infty} (a_k r^k + b_k r^{-k})(c_k \cos k\phi + d_k \sin k\phi) \tag{3.3}$$

A unique solution is available through the application of the boundary condition connecting the inside of the cylinder to the outside of the cylinder.

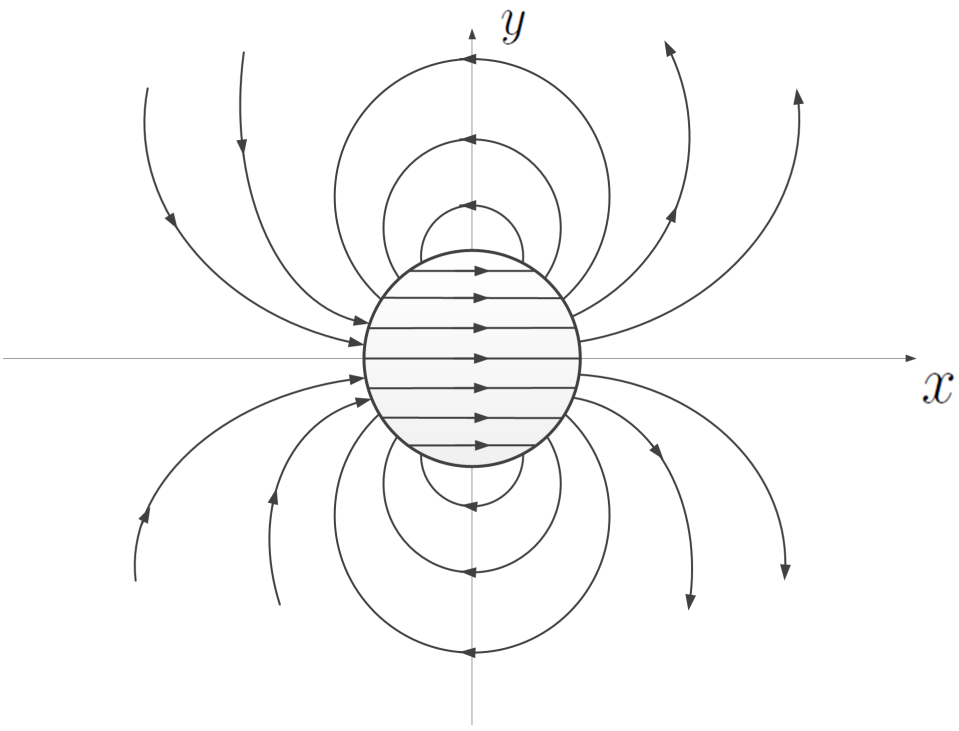

Figure 6: Diagram showing magnetic field lines inside and outside the radius R_{in} of the cosine theta coil

$$(\boldsymbol{H}_{in} - \boldsymbol{H}_{out}) \times \hat{\boldsymbol{r}} = \boldsymbol{k} \qquad r = R_{in} \tag{3.4}$$

One finds interior and exterior solutions

$$U_{in} = -\frac{kr}{2}\cos\phi \qquad\qquad U_{out} = \frac{kR_{in}^2}{2r}\cos\phi \tag{3.5}$$

and leading to magnetic fields given by

$$\boldsymbol{H}_{in} = \frac{k}{2}[cos\phi\,\hat{\boldsymbol{r}} - \sin\phi\,\hat{\boldsymbol{\phi}}] \qquad\qquad \boldsymbol{H}_{out} = \frac{kR_{in}^2}{2r^2}[\cos\phi\,\hat{\boldsymbol{r}} + \sin\phi\,\hat{\boldsymbol{\phi}}] \tag{3.6}$$

A graphical depiction of the magnetic fields is shown in figure 6.

The interior solution is the required constant magnetic field $\boldsymbol{H}_{in} = H_x\hat{\boldsymbol{x}}$. The exterior field might be referred to as a dipole field per unit length of z-axis and falling off as r^{-2}. It is a simple matter to verify that both fields have zero divergence and also satisfy equation (3.4).

A real cosine-theta coil will be characterized by an integer N equal to the total number of wires routed along the surface of the coil. The separation Δx between adjacent wires around the perimeter is constant and has a value

$$\Delta x = \frac{4R_{in}}{N} \tag{3.7}$$

The magnetic field in the interior region follows by summing the contribution to the field from each of the N wires. At the center of the cylinder the magnitude of the field can be written

$$H_x = \frac{I}{2\pi R_{in}^2}\sum_{i=1}^{N}\|y_i\| \tag{3.8}$$

where $\|y_i\|$ is the vertical distance of each wire from the x-axis. Now consider the quantity

$$H_x \cdot \Delta x = \frac{I}{2\pi R_{in}^2}\left[\sum_{i=1}^{N/2} 2\|y_i\| \cdot \Delta x\right] \tag{3.9}$$

But if N is large, the term in parenthesis is a good approximation to the area of the circle, or πR_{in}^2. Now insert equation (3.7) and this derives an approximate formula for H_x in terms of the number N. More generally, the fundamental relation

$$4kR_{in} = NI \tag{3.10}$$

implies that the fields of a cosine theta coil composed of N wires around ($N/2$ current loops) are

$$\boldsymbol{H}_{in} = \frac{NI}{8R_{in}}[cos\phi\,\hat{\boldsymbol{r}} - \sin\phi\,\hat{\boldsymbol{\phi}}] \qquad\qquad \boldsymbol{H}_{out} = \frac{NIR_{in}}{8r^2}[\cos\phi\,\hat{\boldsymbol{r}} + \sin\phi\,\hat{\boldsymbol{\phi}}] \tag{3.11}$$

3.3 Fields of a Double Cos-theta Coil

A theory of a ***double cos-theta coil*** follows from the introduction of a second cosine-theta coil— concentric with the first coil and having a radius R_{out}. The fields of this design are illustrated in figure 7 and show the primary purpose of ensuring that the field external to both coils is zero. With this requirement the current densities $\boldsymbol{k}_1(\phi)$ and $\boldsymbol{k}_2(\phi)$ will necessarily point in opposite directions along the z-axis so that scalar potentials associated with each coil are:

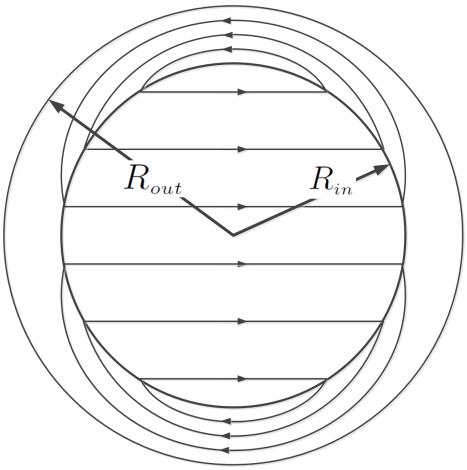

Figure 7: External field lines of a double cosine theta coil with the requirement of no external field. Field lines from the inner coil get squeezed in between R_{in} and R_{out}.

$$U_{1in} = -\frac{k_1 r}{2}\cos\phi \qquad r \le R_{in} \qquad U_{1out} = \frac{k_1 R_{in}^2}{2r}\cos\phi \qquad r > R_{in} \tag{3.12}$$

$$U_{2in} = \frac{k_2 r}{2}\cos\phi \qquad r \le R_{out} \qquad U_{2out} = -\frac{k_2 R_{out}^2}{2r}\cos\phi \qquad r > R_{out} \tag{3.13}$$

Cancellation of the field in the region $r > R_{out}$ requires that current densities and individual radii to be connected by the formula

$$k_1 R_{in}^2 = k_2 R_{out}^2 \tag{3.14}$$

In addition to this, the magnitude of the interior field will be

$$H_{rf} \equiv \frac{1}{2}(k_2 - k_1) \tag{3.15}$$

Both of these equations can be written in terms of coils composed of N_1 and N_2 wires. Specifically,

$$N_1 R_{in} = N_2 R_{out} \qquad\qquad H_{rf} \equiv \frac{I}{8}\left[\frac{N_1}{R_{in}} - \frac{N_2}{R_{out}}\right] \tag{3.16}$$

Potentials for the coil in the two non-zero regions can now be written

$$U_{in}(r,\phi) = -H_{rf} r\cos\phi \qquad\qquad r \le R_{in}$$
$$U_{out}(r,\phi) = \left[\frac{R_{in}^2}{R_{out}^2 - R_{in}^2}\right] H_{rf} \left[r + \frac{R_{out}^2}{r}\right]\cos\phi \qquad\qquad R_{in} < r < R_{out}$$

As before, the auxillary field follows from $\boldsymbol{H} = -\boldsymbol{\nabla} U$. Inside the inner cylinder the field is constant and transverse to the axis of the cylinder so that $\boldsymbol{H}_{in} = H_{rf}\hat{\boldsymbol{x}}$. In the outer region the field is more complicated and given by

$$\boldsymbol{H}_{out}(r,\phi) = \frac{R_{in}^2}{R_{out}^2 - R_{in}^2} H_{rf}\left[-\left(1 - \frac{R_{out}^2}{r^2}\right)\cos\phi\,\hat{\boldsymbol{r}} + \left(1 + \frac{R_{out}^2}{r^2}\right)\sin\phi\,\hat{\boldsymbol{\phi}}\right] \qquad (3.17)$$

It is a simple matter to show that $\boldsymbol{\nabla}\cdot\boldsymbol{H} = 0$ in both regions. Current densities can

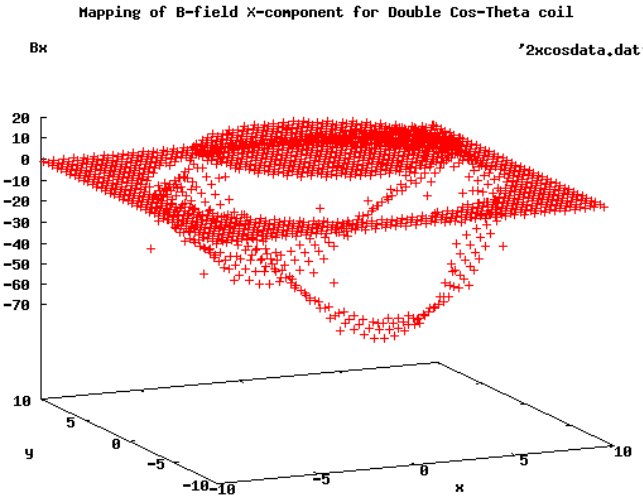

Figure 8: Computer simulation of the x-component of $\boldsymbol{H}$ for the double cosine-theta coil. The field is complicated between the coils but is constant in the interior and zero for all points outside the coil.

also be derived from equations similar to (3.4).

3.4 Inductance of Cosine-Theta Coils

For the theoretical infinite length coils, the meaningful quantity to calculate is the inductance per unit length. It will be more useful however to consider the more realistic problem of a coil with length z_o.

Indutance of a Cosine-Theta Coil: For a coil composed of N wires there are $N/2$ current loops and the total flux thru the coil is given by

$$\Phi = \sum_{i=1}^{N/2} \Phi_i = LI \tag{3.18}$$

The flux thru each current loop is given by the surface integral

$$\Phi_i = \int_s \mathbf{B} \cdot d\mathbf{S}_i \tag{3.19}$$

but the magnetic field is constant in this region and points in the same direction as $d\mathbf{S}$, so

$$\Phi_i = B_x \cdot S_i = \mu_o H_x \cdot S_i \tag{3.20}$$

where S_i is the area enclosed by each loop. The total inductance is therefore

$$\Phi = \mu_o H_x \sum_{i=1}^{N/2} S_i \tag{3.21}$$

and is proportional to the total area enclosed by the individual wire loops. Consider instead the quantity

$$\Phi \cdot \Delta x = LI \cdot \Delta x = \mu_o H_x z_o \left[\sum_{i=1}^{N/2} 2\|y_i\| \cdot \Delta x \right] \tag{3.22}$$

which can be compared to equation (3.9). Again, the value in parentheses approximates the area of the circle of radius R_{in}. Using equation (3.9) the inductance of the cosine-theta coil is

$$\boxed{L = \frac{\mu_o \pi z_o}{32} N^2} \tag{3.23}$$

This same result also follows from a determination of the total energy stored in the magnetic field. The energy inside the coil follows immediately as

$$E_{in} = \frac{\mu_o \pi z_o}{2} \left[\frac{NI}{8} \right]^2 \tag{3.24}$$

The stored energy outside the coil gives the same result. Now write

$$E_{total} = 2E_{in} = \frac{1}{2} LI^2 \tag{3.25}$$

and solve for the inductance.

Inductance of a Double Cosine-Theta Coil: The inductance of a double cosine-theta coil is a more difficult problem to address then a cosine-theta coil. For definiteness it will be assumed here that a double cosine-theta coil is defined by the requirement of a zero external field everywhere. This is an importnat constraint on the radii and the number of wires, and simplifies the calculation.

The total magnetic field energy in the coil in each of two regions is given by

$$E = \frac{\mu_o}{2} \int |\boldsymbol{H}|^2 dv \tag{3.26}$$

In the region $r \leq R_{in}$ the answer is almost trivial since the field is constant. One finds

$$E_{in} = \frac{\mu_o}{2} H_{rf}^2 \pi R_{in}^2 z_o \tag{3.27}$$

In the region $R_{in} < r < R_{out}$ the integral is somewhat more complicated with the result

$$E_{out} = \frac{\mu_o \pi H_{rf}^2 z_o}{2} \left[\frac{R_{in}^2}{R_{out}^2 - R_{in}^2} \right]^2 \cdot \left[\frac{R_{out}^4}{R_{in}^2} - R_{in}^2 \right] \tag{3.28}$$

Now use

$$E_{in} + E_{out} = \frac{1}{2} L I^2 \tag{3.29}$$

and solve the for the inductance.

$$L = \mu_o \pi R_{in}^2 z_o \cdot \frac{H_{rf}^2}{I^2} \left[\frac{2R_{out}^2}{R_{out}^2 - R_{in}^2} \right] \tag{3.30}$$

To complete the calculation it is necessary to insert both of equation of (3.16) so that L appears in terms of geometric quantities only. A symmetric form of the final result is

$$\boxed{L = \frac{\mu_o \pi z_o}{32} N_1 N_2 \left[\frac{R_{out}}{R_{in}} - \frac{R_{in}}{R_{out}} \right]} \tag{3.31}$$

Inductance of the n^{3}He Double Cosine-Theta Coil: The overall design initiative for the n^{3}He double cosine-theta coil is to have every 5th wire routed along the perimeter at R_{in} to be routed along the end faces of the inner cylinder. This condition locks in the ratio of the two radii and the two numbers N_1 and N_2 through the relation

$$\frac{R_{out}}{R_{in}} = \sqrt{\frac{5}{3}} = \frac{N_1}{N_2} \tag{3.32}$$

Actual values for these quantities along with the coil length are given in table 1. Inserting values into equation (3.31), gives an inductance of

$$L = 2.01265 \text{ mH} \tag{3.33}$$

This value is in excellent agreement with experimentally measured values obtained from resonance curves using a known capacitance.

No.	Length
$N_1 = 320$	$R_{in} = 6.320\,\text{in.}$
$N_2 = 248$	$R_{out} = 8.159\,\text{in.}$
	$z_o = 15.60\,\text{in.}$

Table 1: Specifications for the n^3He double cosine-theta coil

Independent Evaluation of L: Inductance of the double cosine-theta coil using specifications in Table 1 can also be deterimined from a good understanding of the derivation for the cosine-theta coil given previously. The total flux thru the inner cylinder is

$$\Phi = \mu_o H_{rf} \sum_{i=1}^{N/2} S_i \tag{3.34}$$

which is identical to equation (3.21) except that H_x has been replaced by the quantity H_{rf}. Solving for the quantity L_{in} in the same manner gives

$$L_{in} = \frac{\mu_o H_{rf} \pi R_{in}^2 z_o}{I \cdot \Delta x} \tag{3.35}$$

But equation (3.32) can be inserted into equation (3.16) to show that

$$\frac{H_{rf}}{I} = \frac{1}{\Delta x} = \frac{N}{4R_{in}} \tag{3.36}$$

where $N = 64$ for the inner cylinder. The final result is

$$L_{in} = \frac{\mu_o \pi z_o N^2}{16} \tag{3.37}$$

which is double the result for a cosine-theta coil. To determine the contribution from outer cylinder loops it is only necessary to note that the total flux through the top half of the inner cylinder runs entirely through the top half of the outer cylinder. The only difference is that this flux traverses four times as many wire loops. This means that $L_{out} = 4 \cdot L_{in}$. The total inductance for the n^3He coil is therefore

$$\boxed{L = \frac{5}{16} \mu_o \pi z_o N^2} \tag{3.38}$$

This is a useful formula for L given exclusively in terms of the number of wires routed along the inner cylinder.

3.5 Spin Flipper and Spin Magnetic Resonance

The rotation of neutron spins inside the spin flipper is easily decribed by the classic two state problem of Spin Magnetic Resonance (SMR). Spins emerging from the Super Mirror Polarizer are initially polarized along the direction of the magnetic holding field $\boldsymbol{B}_o$ which has a magnitude of 9.134 Gauss. Figure 9 shows these vectors along with the transverse field $\mathbf{B}_{rf}$ produced by the spin flipper. The neutron has a

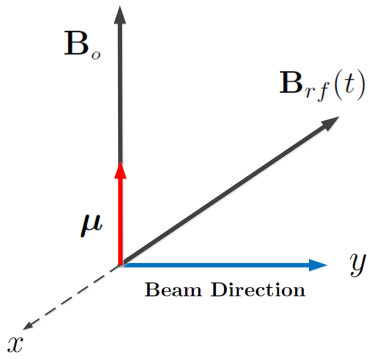

Figure 9: Magnetic field vectors. The direction of $\mathbf{B}_{rf}$ oscillates in the horizontal plane at 26.6 kHz.

magnetic moment

$$\mu = g_n \mu_n = -1.9130427 \mu_n \tag{3.39}$$

where g_n is the spin g-factor and where μ_n is the nuclear magneton given by

$$\mu_n = e\hbar/2m_p = 5.050783 \times 10^{-27} \mathrm{J/T} \tag{3.40}$$

The neutron gyromagnetic ratio is determined beginning with the general equations

$$E = -\boldsymbol{\mu} \cdot \mathbf{B} \qquad\qquad \boldsymbol{\mu} = g_n \frac{e}{m_p} \mathbf{S} \tag{3.41}$$

For neutrons inside an energized spin flipper, the magnetic moment interacts with the total field

$$\mathbf{B} = B_o \hat{\boldsymbol{z}} + B_{rf} \cos \omega t \hat{\boldsymbol{x}} \tag{3.42}$$

and this field defines two frequencies

$$\omega_L \equiv \gamma_n B_o \qquad\qquad \omega_F \equiv \gamma_n B_{rf} \tag{3.43}$$

The first frequency is the Larmor frequency of neutrons in the holding field which translates to a Larmor precession frequency of

$$\nu_L = 26.6390298 \,\mathrm{kHz} \tag{3.44}$$

The second frequency is specifically associated with the RF field and the number γ_n is the gyromagnetic ratio given by

$$\gamma_n = g_n \frac{e}{m_p} = 1.83247165 \times 10^8 \frac{1}{sT} \tag{3.45}$$

When the spin flipper is off, the initial quantum mechanical hamiltonian for the neutrons interacting with the holding field is represented by the simple two state matrix

$$H = \begin{bmatrix} \frac{\hbar\omega_L}{2} & 0 \\ 0 & -\frac{\hbar\omega_L}{2} \end{bmatrix} \tag{3.46}$$

and the initial spin state $|\psi>$ for the beam is derived from a knowledge the initial beam polarization of approximately 95%.

The entrance of the neutrons into the interior region of the spin flipper marks the presence of a time-dependent perturbing potential energy which modifies the off-diagonal elements of the two state hamiltonian leading to

$$H \rightarrow \frac{\hbar}{2} \begin{bmatrix} \omega_L & 4\omega_F e^{i\omega t} \\ 4\omega_F e^{-i\omega t} & -\omega_L \end{bmatrix} \tag{3.47}$$

and where $\omega_F << \omega_L$. In general, the frequency of the perturbing potential can be anything but to rotate neutron spins by 180 degres with a probability approaching 1, it is necessary to drive the spin flipper at resonance where $\omega \rightarrow \omega_L$. At this frequency, the probability of finding neutrons in the spin flipped state derives from the Rabi formula and is given by

$$P(-1) = \sin^2(2\omega_F t) \tag{3.48}$$

For neutrons of specific energy E, this means we choose ω_F based on the total time δt these neutrons are exposed to the RF field. The angular frequency (rate of neutron flip) must be

$$\omega_F = \pi/\delta t \tag{3.49}$$

but since the spin flipper is characterize by a field which will oscillate at frequency ω_L (i.e not constant and not rotating at this frequency) then the appropriate equation for the RF magnetic field will be

$$\boxed{B_{rf}(t) = \frac{2\omega_F}{\gamma_n} \cdot e^{i\omega_L t}} \tag{3.50}$$

Table 2: Table

No.	λ	velocity(v_n)	δt
1	$6.5A$	608.620 m/s	0.6510 ms
2	$5.0A$	791.205 m/s	0.5008 ms
3	$3.5A$	1,130.294 m/s	0.3505 ms
4	$2.5A$	1,582.411 m/s	0.2504 ms

SMR for a Wavelength Spectrum: The flux of neutrons through the spin flipper is actually composed of a distribution of de Broglie wavelengths in the approximate range $2.5A \leq \lambda \leq 6.5A$. For reference, Table 2 gives an indication of selected neutron velocities in this range along with the total time spent inside the spin flipper. The length of the spin flipper is 39.62 cm.

The angular rate of neutron flip is given by equation (3.49) and this means that ω_F will depend on the wavelength of the neutron according to

$$\omega_F = \frac{\pi h}{z_o m \lambda} \tag{3.51}$$

For a given pulse of neutrons, the amplitude of the RF field inside the spin flipper

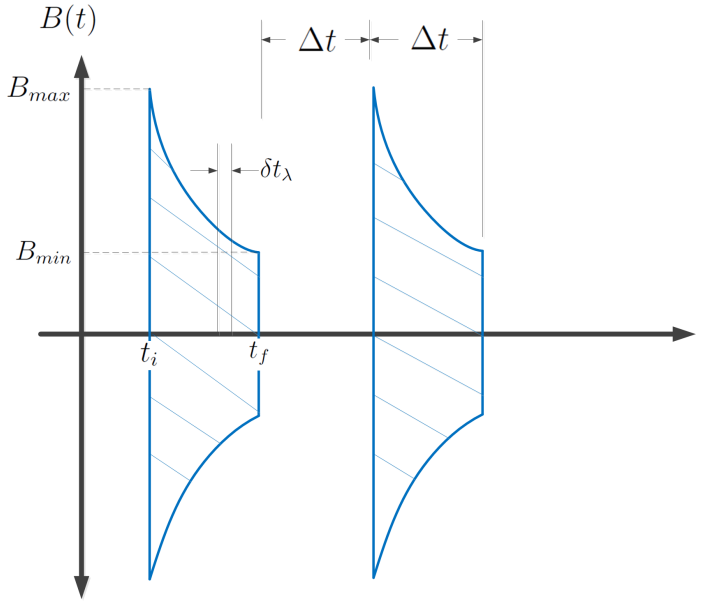

Figure 10: Magnetic field envelope provided by the spin flipper. The region of zero field between the pulses transmits neutrons without flipped spins.

will therefore be required to decrease with a $1/t$ dependence over a time interval Δt

and having the general form

$$B_{rf}(t) = \frac{B_{max}}{t} e^{i\omega_L t} \tag{3.52}$$

An example plot of the RF field envelope provided by the spin flipper is shown in Figure 10. The spin flipper triggers-on at time t_i simultaneous with the arrival of the front of the pulse and then triggers-off at a time t_f later. The SNS provides pulses of neutrons at 60 Hz implying that that the width of a pulse is

$$\Delta T = t_f - t_i = 16.67\,\text{ms} \tag{3.53}$$

The fastest neutrons will be located at the front of the pulse and recieve that portion of the RF field with the largest amplitude. In contrast, the slowest neutrons are at the back of the pulse and recieve the smallest field amplitude. The total time spent by any neutron in the spin flipper is δt_λ which is much smaller than the width of the pulse.

3.6 RF Power Requirements for the Spin Flipper

The double cosine-theta coil of the spin flipper has an inductance L and resistance R based on the total length of wire used. Under an applied AC voltage it behaves as an LR circuit. However, the n^{3}He experiment will require an RF field to rotate neutron spins and this means that an external capacitor will be required so that the spin flipper can be driven as an RCL circuit. A schematic of the circuit is shown in Figure 11. The required RF frequency is the Larmor frequency ω_L of neutrons in the

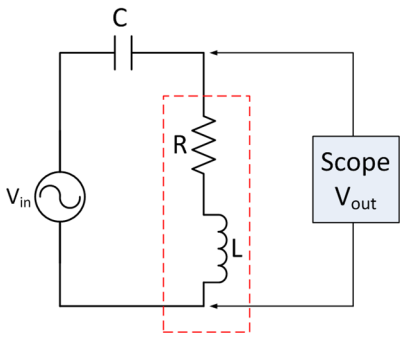

Figure 11: The spin flipper is represented by the red dashed line. An appropriately chosen external capacitance must be added separately.

external holding field of the experiment. The inductance of the double cosine-theta coils has also been calculated previously and the capacitance is easily determined as

$$C = 1/\omega_L^2 L \sim 17.70\,\text{nF} \tag{3.54}$$

The only other information needed for the RCL circuit is the resistance R of the spin flipper which is determined by the 870 length of wire and the resistivity of aluminum. For convenience, values of all circuit elements are summarized in Table 3:

R	C	L
$9.11\,\Omega$	$17.70\,\mathrm{nF}$	$2.01\,\mathrm{mH}$

Table 3: Values of passive circuit elements for the spin flipper

Power Formula: With an applied external voltage $V(t) = V_o e^{i\omega_L t}$, the steady state differential equation for the spin flipper circuit can be written in terms of the charge $Q(t)$ on the capacitor:

$$L\frac{d^2Q}{dt^2} + R\frac{dQ}{dt} + \frac{Q}{C} = V_o e^{i\omega_L t} \tag{3.55}$$

Differentiating the well known solution to this equation leads to the current formula

$$I(t) = \frac{V_o}{\left[R^2 + (\omega L - \frac{1}{\omega C})^2\right]^{1/2}} \cdot \sin(\omega t + \phi) \tag{3.56}$$

and the average power supplied to the circuit over one cycle is $P_{avg} = \frac{1}{2} I_\omega^2 R$ or

$$P_{avg} = \frac{V_o^2 R/2}{R^2 + (\omega L - \frac{1}{\omega C})^2} \tag{3.57}$$

If the spin flipper is operated at resonance then $V_o = IR \approx 5.0$ Volts and

$$P_{avg} = \frac{V_o^2}{2R} \approx 1.4\,\mathrm{Watts} \tag{3.58}$$

Resonance Curve: An important indicator for any RCL circuit is its Q-value which is defined by the relation:

$$Q = \omega_L \cdot \frac{\text{Total stored energy}}{\text{Average power supplied at resonance}} \tag{3.59}$$

For the spin flipper:

$$Q = \frac{\omega_L L}{R} \approx 37.2 \tag{3.60}$$

This is a large value and qualifies the spin flipper as an underdamped oscillator. It can also be approximated from the resonance curve shown in Figure 12. Individual points on this curve were made available using a small probe placed near the center of the spin flipper and attached to an SR860 lock-in amplifier. The precise measurements

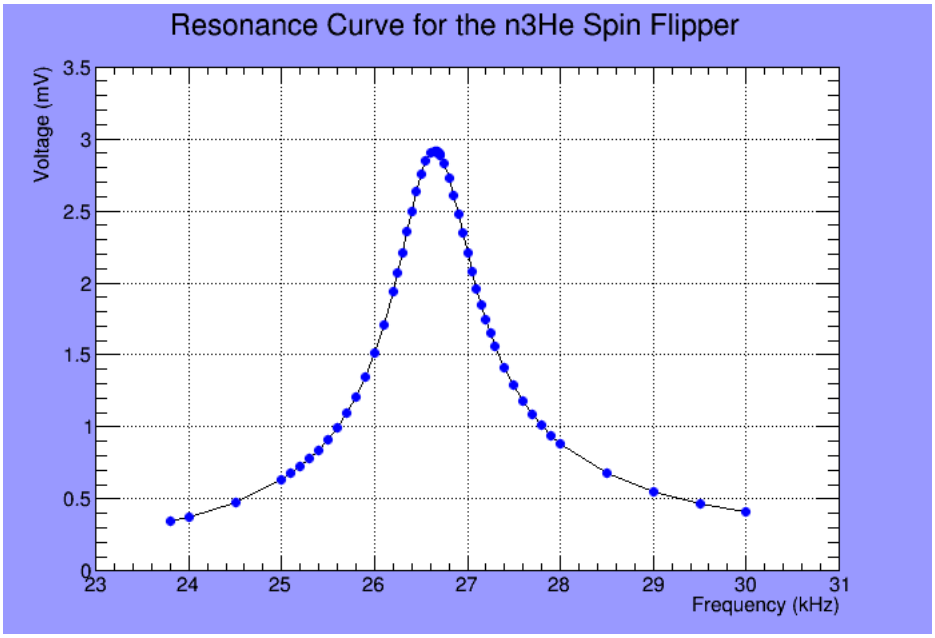

Figure 12: Resonance Curve

required matching the frequency on the lock-in amplifier with the driving frequency of the function generator. Characteristics of the curve are

$$V_{max} = 2.916\,\text{mV} \;@\; f = 26.655 \pm 0.005\text{kHz} \qquad \text{FWHM} \approx 1.4\text{kHz} \tag{3.61}$$

The Q-value can be determined from the curve from the quantity $f/\Delta f$ where Δf is half of the FWHM.

4 Polarimetry for the n^{3}He Experiment

Polarimetry measurements on the neutron beam are an essential part of the n^{3}He experiment for several reasons: The statistical evaluation of the constant A_p requires that a large beam polarization be maintained and it is therefore necessary to report on beam polarization at various time intervals during the experiment. Equally important are interim checks to verify proper tuning of the external holding field to the spin flipper.

It is expected that polarimetry measurements will be conducted 4-5 times during the course of the experiment with mandatory measurements before and after the production of data. A polarimetry measurement will consist of the following:

- Measurement of the polarization $P_n(\lambda)$ of the neutron beam transmitted by the Super Mirror Polarizer as a function of wavelength.

- Measurement of the efficeincy $\epsilon_{sf}(\lambda)$ of the spin flipper as a function of neutron wavelength.
- Optimization of the Spin Flip Ratio to ensure proper tuning of the external magnetic holding field. A tuned holding field maximizes spin flipper efficiency and minimizes de-polarization thru the Spin flipper.

The polarization of the neutron beam and the spin flipper efficiency can be measured redundantly at two different ^{3}He cell polarizations to ensure a correct analysis. The optimization curve reulting from the third bulleted item can be measured at three or more perturbations of the magnetic holding field. Minimum values for a succesful statistical result for the n^{3}He experiment are

$$\bar{P}_n > 95\% \qquad\qquad \bar{\epsilon}_{sf} > 98\% \tag{4.1}$$

where the overbar indicates an average over the wavelength range of approximetely 3.0 - 6.5A. There is little reason to believe that initial values of beam polarization and spin flipper efficiency will change much during the experiment. However, any values for these two quantities which are out of specification must be reported immediately.

4.1 Fundamentals of Neutron Polarimetry

The ability to perform accurate polarimetry measurements for the n^{3}He experiment requires knowledge of the science of neutron polarimetry. The spin filter is a glass cell filled with ^{3}He so the essential problem will be to understand what happens to a beam of neutrons upon transmission thru a gas of either polarized, or unpolarized ^{3}He.

Properties of a ^{3}He Spin Filter: A ^{3}He spin filter can also be referred to as an *analyzer cell* or a ^{3}He *cell*. Nuclear spins of ^{3}He atoms inside the cell can be polarized using the technique of *Spin Exchange Optical Pumping(SEOP)*, and a significant portion of the initial polarization can be maintained for a period of several days in a uniform holding field. This property when coupled with the very strong spin-dependent capture cross section make a ^{3}He cell ideal for performing polarimetry measurements on a beam of cold neutrons.

The capture cross-section for cold neutrons in a ^{3}He cell can be modeled as a linear function of wavelength as long as the wavelengths are not too small:

$$\sigma(\lambda) \sim \frac{\sigma_o}{\lambda_o}\,\lambda \tag{4.2}$$

The ratio of the constants σ_o and λ_o represent an instrinsic property of the cell representing its ability to capture neutrons. The likely cell for the n^{3}He experiment will be "Hedy Lamarr" discussed in [9], and characterized by

$$\sigma_o = 5316\,\text{bn} \qquad\qquad \lambda_o = 1.798\,A \tag{4.3}$$

Other important dimensions are its diameter $d = 7.5$ cm and its length $\ell = 10.3$ cm. The *Cell Thickness* is defined by the equation

$$\chi \equiv \frac{n\sigma_o \ell}{\lambda_o} \tag{4.4}$$

where n is the number density of atoms in the cell. Using a known value of $\chi = 1.004$ implies that Heddy Lamar has a ^{3}He number density of

$$n = 3.396 \times 10^{25} \text{ atoms}/m^3$$

Transmission of Unpolarized Neutrons through an Unpolarized Cell: Now suppose a flux $T_o(\lambda)$ of unpolarized neutrons is incident on an unpolarized cell. Omitting a formal derivation, the percentage of transmitted neutron flux is known to be

$$T(\lambda) = T_o(\lambda)e^{-\chi\lambda} \tag{4.5}$$

The function $T_o(\lambda)$ is a density function characteristic of the pulsed source at the

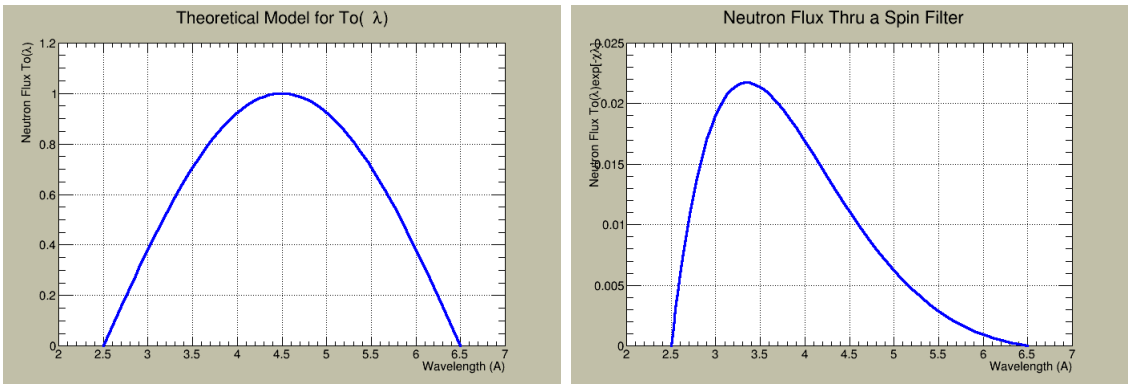

Figure 13: A model for a neutron beam flux over a wavelength range 2.5-6.5 Angstroms and the resulting transmission emerging from the cell

SNS but it will suffice to consider a simple model for $T_o(\lambda)$ having the form

$$T_o(\lambda) = \sin\left[\frac{\pi}{4}(\lambda - 2.5)\right] \tag{4.6}$$

Figure 13 shows a plot of this function on th left and also shows the flux emerging from the unpolarized cell on right. Of particular interest is the observation that transmitted flux is relatively small compared to the intial flux indicating that the cell has absorbed most of the neutrons. In addition to this the distribution is skewed in favor of smaller wavelengths. The argument here is that smaller wavelengths imply faster neutrons which spend less time in the cell and therefore have a smaller probability of being absorbed. It is important to mention that the transmittance of the beam thru the cell is independent of the initial polarization of the beam. A beam polarized in an arbitrary direction will transmit just as many neutrons as an unpolarized beam. This is only true if the cell is unpolarized.

Transmission of Unpolarized Neutrons thru a Polarized Cell: A more interesting problem is an unpolarized neutron beam incident on a ^{3}He cell having a polarization P. The initial beam can be thought of as having equal numbers of neutrons parallel and anti-parallel to the polarization direction of the cell. The transmission of each component can be written

$$T_{pa}(\lambda) = \tfrac{1}{2}T_o(\lambda)e^{-\chi\lambda(1-P)} \qquad\qquad T_{ap}(\lambda) = \tfrac{1}{2}T_o(\lambda)e^{-\chi\lambda(1+P)} \tag{4.7}$$

and the total transmission thru the cell is

$$T(\lambda) = T_{pa} + T_{ap} = T_o(\lambda) \cdot e^{-\chi\lambda}\cosh(\chi\lambda P) \tag{4.8}$$

For reference, figure 14 shows a plot of the transmission of each component for a cell polarized to $P = 0.5$. Once again, the presence of the cell eliminates a large portion of the initial beam but the transmission of spins parallel to the polarization direction of the cell is much larger than anti-parallel spins.

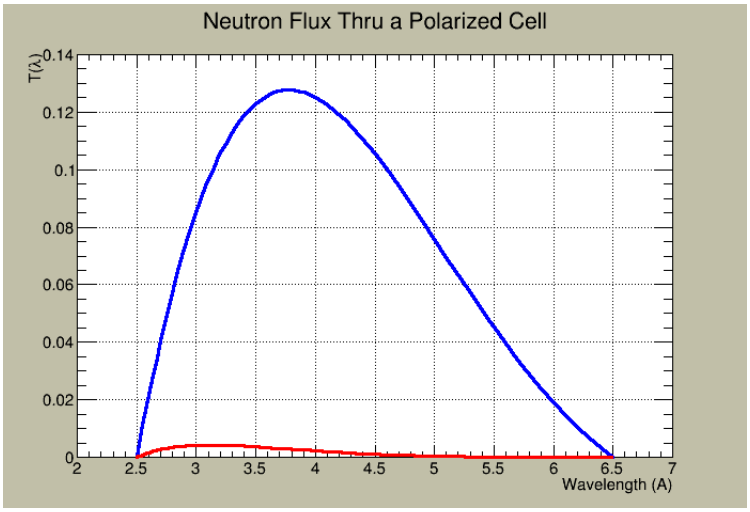

Figure 14: Transmission of individual components of an unpolarized beam thru a polarized cell. Parallel component in blue and anti-parallel component in red.

An important calculation is the polarization of the beam after transmission thru the cell:

$$P_n(\lambda) = \frac{T_{pa} - T_{ap}}{T_{pa} + T_{ap}} = \tanh(\chi\lambda P) \tag{4.9}$$

Since the initial beam is unpolarized, the quantity $P_n(\lambda)$ can be referred to as the *analyzing power* of the cell at wavelength λ—a measure of the ability of the cell to polarize the beam.

Transmission of Polarized Neutrons thru a Polarized Cell: Now suppose the initial neutron beam polarization is $P_n(\lambda)$. The transmitted beam flux through the cell for parallel and anti-parallel components of the beam is

$$T_{pa}(\lambda) = \tfrac{1}{2} T_o(\lambda)\,[1 + P_n]\, e^{-\chi\lambda(1-P)} \tag{4.10}$$

$$T_{ap}(\lambda) = \tfrac{1}{2} T_o(\lambda)\,[1 - P_n]\, e^{-\chi\lambda(1+P)} \tag{4.11}$$

and the total transmission through the cell can be written

$$T(\lambda) = T_{pa}(\lambda) + T_{ap}(\lambda) = T_o(\lambda) \cdot e^{-\chi\lambda}\,[\cosh(\chi\lambda P) + P_n \sinh(\chi\lambda P)] \tag{4.12}$$

By setting $P \to 0$ in this formula, the transmission through an unpolarized ^{3}He cell is recovered. This may be considered as a proof that transmission through an unpolarized cell is independent of the initial beam polarization.

When both the beam and the cell are polarized it is convenient to consider separate cases where the beam polarization is either parallel or anti-parallel to the cell polarization. Plots for both cases are shown in figure 15 assuming a typical BL-13 initial polarization of $P_n = 0.95$ and a cell polarization of $P = \pm 0.5$. From the plots

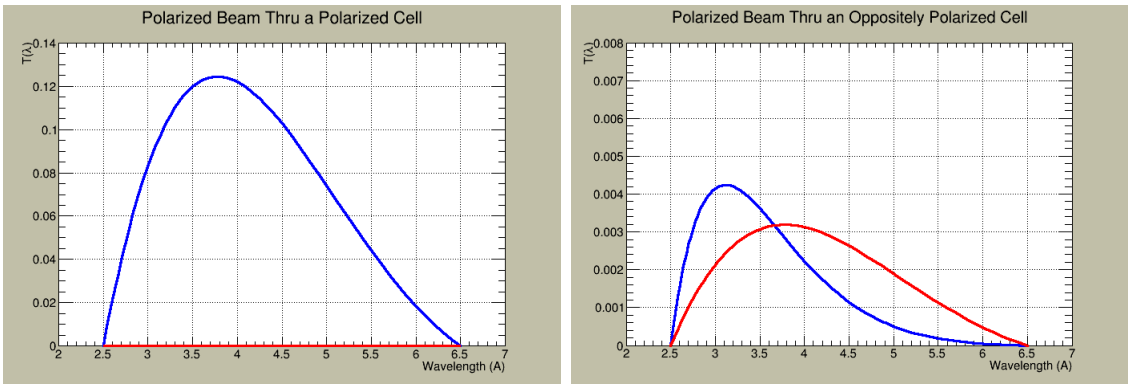

Figure 15: Transmission of individual beam components for beam polarization parallel and and anti-parallel to cell polarization.

it is evident that when the beam polarization is parallel to the cell polarization, there exists a large transmitted parallel component while the anti-parallel component is virtually non-existent. In contrast, if the beam and cell polarization are anti-parallel both components are highly supressed.

A calculation of the polarization of the emerging beam shows that

$$P_n'(\lambda) = \frac{\tanh(\chi\lambda P) + P_n}{1 + P_n \tanh(\chi\lambda P)} \tag{4.13}$$

and this is plotted in figures 16. For parallel beam and cell polarizations the emerging beam is almost completely polarized. When the polarizations are antiparallel, the polarization of the emerging beam is dependent on the wavelength of the transmitted neutrons.

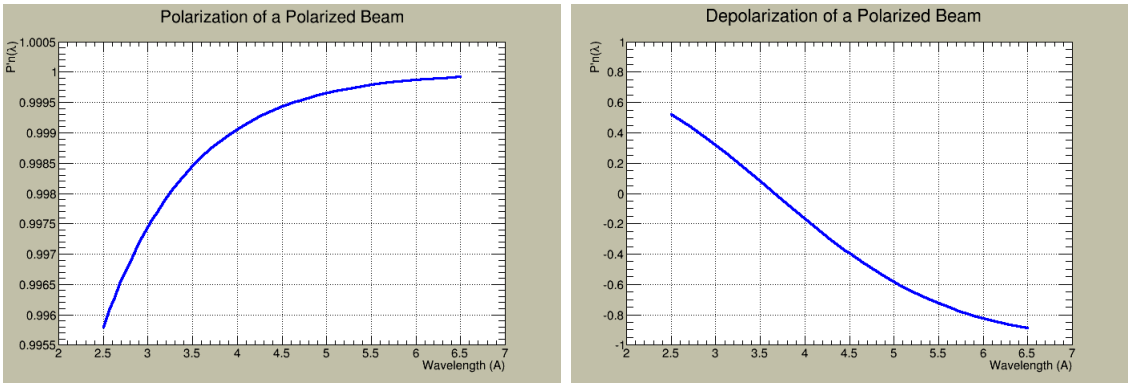

Figure 16: Plots showing emerging polarization of a beam when beam and cell polarizations are (1) parallel, and (2) anti-parallel.

4.2 Polarimetry with a Spin Flipper

Fundamental polarimetry presented thus far assumes only the existence of a beam and a ^{3}He cell—either of which may be polarized or unpolarized. However, the initial beam has a large polarization from a super mirror polarizer approaching 95%. Moreover, the spin flipper is an integral part of the experiment which is capable of reversing the polarization of the beam at a rate of approximately 500 times a second. It can be used as a tool to measure both beam polarization and cell polarization, but also has the internal property of spin flip efficiency ϵ_{sf} which must be measured since its value is an important statistical parameter in the experiment.

Calculation of Beam Polarization: The polarization $P_n(\lambda)$ of the neutron beam can be determined from independent measurements with a polarized cell and an unpolarized cell. The transmission thru an unpolarized cell has already been determined to be

$$T_{unp} = T_o(\lambda) \cdot e^{-\chi\lambda} \tag{4.14}$$

The spin flipper can be on or off here since the transmission through the cell favors no direction of the incoming spins. Now suppose transmission measurements are made thru a polarized cell with the spin flipper on and off. Refer to these transmissions as T_{on} and T_{off}, and define relative transmission coefficients R_1 and R_2 by

$$R_1 \equiv \frac{T_{on}}{T_{unp}} \qquad\qquad R_2 \equiv \frac{T_{off}}{T_{unp}} \tag{4.15}$$

For a polarized beam incident on a polarized cell, the total transmission through the cell is given by equation 4.12. If the polarization is reversed by the spin flipper having

an efficiency ϵ_{sf}, then the values of R_1 and R_2 will be

$$R_1 = \cosh(\chi\lambda P) + P_n \sinh(\chi\lambda P) \tag{4.16a}$$
$$R_2 = \cosh(\chi\lambda P) + \alpha P_n \sinh(\chi\lambda P) \tag{4.16b}$$

where $\alpha = 1 - 2\epsilon_{sf}$. Solving for $\cosh(\chi\lambda P)$ in terms of R_1 and R_2 leads to

$$\cosh(\chi\lambda P) = \frac{R_2 - \alpha R_1}{1 - \alpha} \tag{4.17}$$

Now solve equation 4.16a for P_n

$$P_n = \frac{R_1 - \cosh(\chi\lambda P)}{\sinh \chi\lambda p} \tag{4.18}$$

and insert equation 4.17 to determine the formula by which the polarization of the neutron beam can be determined. One finds

$$\boxed{P_n(\lambda) = \frac{R_1 - R_2}{\sqrt{[R_2 - (1 - 2\epsilon_{sf})R_1]^2 - 4\epsilon_{sf}^2}}} \tag{4.19}$$

It is important to observe here that polarization values get smaller as the value of ϵ_{sf} is increased near the value of 1. An approximate formula can be determined in the form

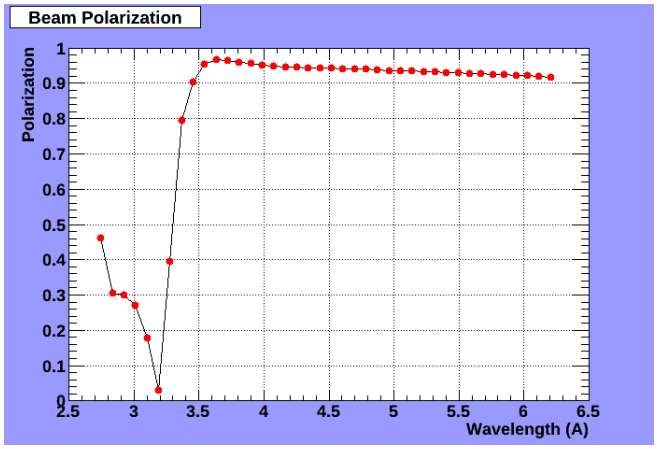

Figure 17: Beam Polarization vs neutron wavelength.

$$P_n = -m\epsilon_{sf} + b \tag{4.20}$$

This means that the effect of excluding spin flipper efficiency in the calculation of beam polarization is to give a result which is somewhat smaller than it actually is.

The model for spectral beam flux in figure 13 predicts a beam polarization which is absolutely independent of wavelength. An actual experimental polarization curve is illustrated in figure 17. The experimental curve is only good for wavelengths greater than about 3.5 Angstroms and the polarization above this value has a small non-zero slope. A useful number here is the average polarization $\bar{P}_n = 0.9338$ from 3.5-6.5 Angstroms.

Calculation of the Spin Flipper Efficiency: The experimental spin flipper efficiency $\epsilon_{sf}(\lambda)$ can be calculated based on transmission measurements of the polarized neutron beam through a polarized ^{3}He cell having spins which can be flipped by Adiabatic Fast Passage (AFP). If the spin flipper is initially off, the total transmission through the cell with polarizations P and $-P$ is

$$T = T_o(\lambda)e^{-\chi\lambda}\left[\cosh(\chi\lambda P) + P_n \sinh(\chi\lambda P)\right] \tag{4.21a}$$

$$T_{afp} = T_o(\lambda)e^{-\chi\lambda}\left[\cosh(\chi\lambda P) - P_n \sinh(\chi\lambda P)\right] \tag{4.21b}$$

which determines the polarization quantity

$$P_{off} = \frac{T - T_{afp}}{T + T_{afp}} = P_n \tanh(\chi\lambda P) \tag{4.22}$$

If the procedure is repeated with the spin flipper turned on equations (4.21) are modified to read:

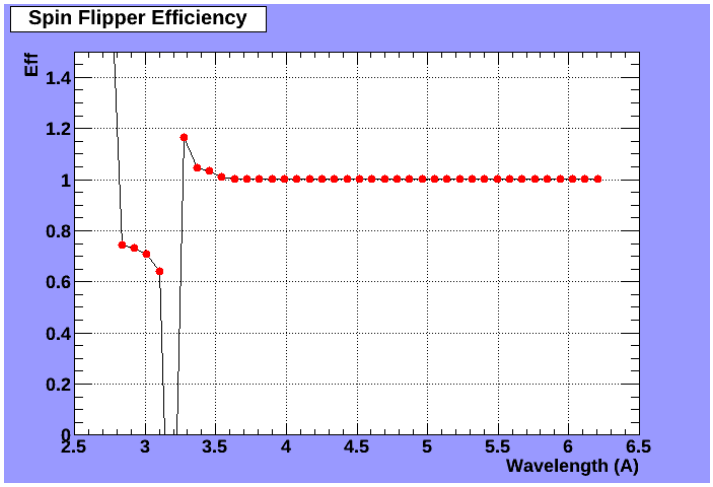

Figure 18: Plot of $\epsilon_{sf}(\lambda)$ for the n^{3}He spin flipper.

$$T = T_o(\lambda)e^{-\chi\lambda}\left[\cosh(\chi\lambda P) + \alpha P_n \sinh(\chi\lambda P)\right] \tag{4.23a}$$

$$T_{afp} = T_o(\lambda)e^{-\chi\lambda}\left[\cosh(\chi\lambda P) - \alpha P_n \sinh(\chi\lambda P)\right] \tag{4.23b}$$

and a new polarization quantity is

$$P_{on} = \frac{T - T_{afp}}{T + T_{afp}} = \alpha P_n \tanh(\chi\lambda P) \tag{4.24}$$

The two values P_{off} and P_{on} are determined from measurable quantities produced by the beam monitor, and they are easily shown to determine the spin flipper efficiency from

$$\epsilon_{sf} = \frac{1}{2}\left[1 - \frac{P_{on}}{P_{off}}\right] \tag{4.25}$$

This calculation initially assumes that the action of the AFP flip does not de-polarize the beam; But realistically, each AFP flip produces a cell de-polarization on the order of a few percent. An easy way to get around this is to perform transmission measurements using an extra AFP flip back to the initial polarization of the cell. One can then average the initial transmission with the transmission following two AFP flips. Formulas for the emerging beam polarization are then modified to read

$$\begin{bmatrix} P_{off} \\ P_{on} \end{bmatrix} = \frac{\bar{T} - T_{afp}}{\bar{T} + T_{afp}} \tag{4.26}$$

Calculation of the Spin Flip Ratio: An important polarimetry measurement is the spin flip ratio which is the ratio of transmitted signals thru a ^{3}He cell from a polarized beam before and after the polarization of the beam is reversed by the spin flipper. The spin flip ratio is very sensitive to the efficiency ϵ_{sf} of the spin flipper. Mathematically, $\mathcal{Q}_{sfr}$ is defined by

$$\mathcal{Q}_{sfr} \equiv \frac{T_{off}}{T_{on}} \tag{4.27}$$

For a polarized beam incident on a cell of polarization P this ratio is determined by equation (4.16)

$$\mathcal{Q}_{sfr} = \frac{R_1}{R_2} = \frac{1 + P_n \tanh(\chi\lambda P)}{1 + \alpha P_n \tanh(\chi\lambda P)} \tag{4.28}$$

If the cell is not polarized then $P = 0$ and the spin flip ratio is 1. An upper limit to $\mathcal{Q}_{sfr}$ is also available by considering large values inside the arguments of the hyperbolic tangents

$$\mathcal{Q}_{sfr}(max) = \lim_{\chi\lambda P \to \infty} \mathcal{Q}_{sfr} = \frac{1 + P_n}{1 + \alpha P_n} \tag{4.29}$$

For a spin flipper efficiency approaching 1 and a beam polarization of 95% this number has a value of about $30 - 40$ with a dependency on the wavelength not indicated by the model. A plot $\mathcal{Q}_{sfr}(\lambda)$ is shown in figure 19 for three different magnetic field settings.

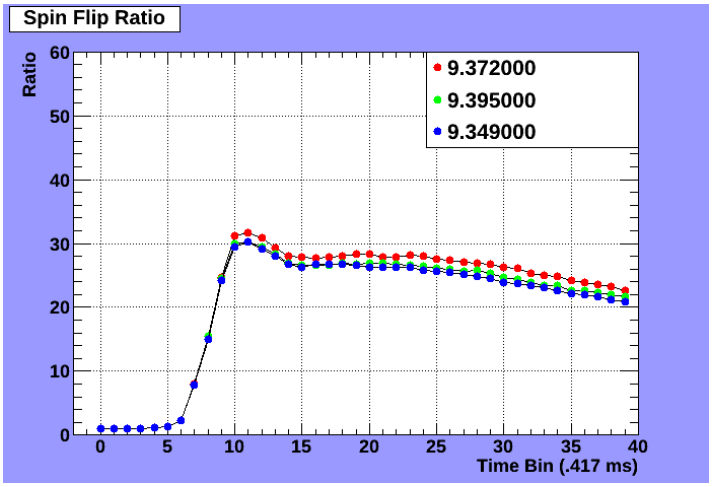

Figure 19: Three plots of Spin Flip Ratio vs time bin for slightly modified values of magnetic field.

The spin flip ratio might also be defined by making transmission measurements before and after reversing the polarization of the ^{3}He cell by AFP flip. The spectral value $\mathcal{Q}_{sfr}(\lambda)$ will certainly be similar to the original spin flip ratio but differences will result because of slight de-polarization of the cell which can be written

$$P \longrightarrow \kappa P \tag{4.30}$$

where $\kappa \sim 0.98$. For this reason only the first definition will be considered.

Tuning the External Field to the Spin Flipper: As already mentioned, one of the primary reasons for performing polarimetry measurements during the n^{3}He experiment is to ensure that the value B_o of the magnetic holding field is properly tuned to the resonant frequency of the spin flipper. Tuning is performed by measuring the spin flip ratio at several values of magnetic field near the value which maximizes $\mathcal{Q}_{sfr}$. The resulting plot is necessarily parabolic and shows the optimal setting for B_o. An example is shown in figure 20. The curve for the optimation is

$$\mathcal{Q}_{sfr} = \mathcal{Q}_{sfr}(max) + C \cdot (B - B_o)^2 \tag{4.31}$$

where B is the tunable magnetic field variable and C is a large negative constant having a value of approximately $500 - 1000\, G^{-2}$. A derivation of this curve is somewhat complicated but can be determined by setting ϵ_{sf} equal to the quantum mechanical Rabi formula

$$\epsilon_{sf} = \frac{\omega_F^2}{\omega_F^2 + (\omega_L - \omega_{rf})^2} \sin^2 \left[\sqrt{\omega_F^2 + (\omega_L - \omega_{rf})^2}\, \frac{t}{2} \right] \tag{4.32}$$

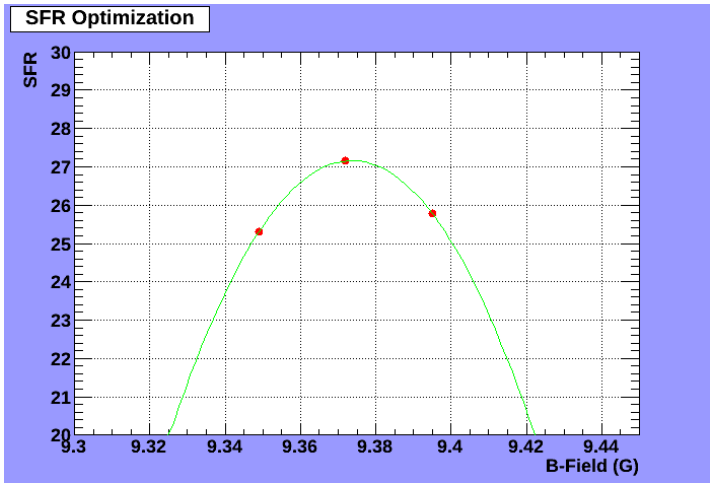

Figure 20: SFR plotted against small deviations of magnetic holding field away from the optimal B_o.

The frequency ω_F is determined by equation (3.51) and represents the rate of neutron flip inside the spin flipper while ω_{rf} is the driven frequency of the RF field inside the spin flipper. The frequency ω_L is the Larmor frequency of neutrons in the holding field and is the variable quantity in the Rabi equation. The efficiency is maximized when $\omega_L \to \omega_{rf}$ so that

$$A(\omega_L) = \frac{\omega_F^2}{\omega_F^2 + (\omega_L - \omega_{rf})^2} \longrightarrow 1 \tag{4.33}$$

and equation (4.31) follows by inserting $A(\omega_L)$ into (4.28) and expanding in terms of the small quantity

$$\delta = (\omega_L - \omega_{rf})/\omega_F \tag{4.34}$$

Concluding Remarks Initial construction of the n^{3}He experiment is nearing completion. Settings for the guide field have been finalized for alignment with the ion chamber. In the coming weeks designers of the experiment are hoping to determine the centroid of the neutron beam by performing XY- beam scans at different locations along the beam; knowledge of the beam centroid should improve overall statistical uncertainty of the experiment. Under ideal conditions the experiment will be in production mode for most of 2015.

References

[1] Bertrand Desplanques, J.F. Donoghue, B.R. Holstein. Unified Treatment of the parity violating nuclear force. Annals of Physics 124(2):449-495, 1980.

[2] G Greene, A K Thompson, M S Dewey. A method for the accurate determination of the polarization of a neutron beam using a polarized ^{3}He spin filter. Nuclear Instruments and Methods in Physcis Research, Section A: Accelerators, Spectrometers, Detectors and associated equipment, 356(2-3):177-180, March 1995.

[3] Matthew Musgrave, The NPDGamma Experiment and Polarimetry using a ^{3}He Spin Filter. Comprehensive Exam Write-up, July 18, 2011.

[4] Mostafa Jon Dadras. Polarimetry Studies for the NPDGamma Experiment at the SNS. Masters Thesis, University of Tennessee, Department of Physics and Astronomy. December 2009.

[5] R. Chad Gillis. ^{3}He Ionization Chambers as Neutron Beam Monitors for the NPDGamma Experiment. Masters Thesis, department of Physics and Astronomy, University of Manitoba, Winnipeg, Manitoba, Canada. June 2006.

[6] Resonant Frequency Neutron Spin Flipper, Double Cosine Theta Coil Winding. Unpublished paper written by Tomy, Graduate student of Chris Crawford. May 10, 2011.

[7] A measurement of the Parity Violating Proton Asymmetry in the Capture of Polarized Cold Neutrons on ^{3}He. A Proposal submitted to the SNS FNPB PRAC. November 15, 2007.

[8] Detector Development for an Experiment to Measure the Parity Violating Proton Asymmetry in the Capture of Polarized Cold Neutrons on ^{3}He. J.D. Bowman, C.B. Crawford, M.T. Gericke et al. March 17, 2008.

[9] Matthew Martin Musgrave. Neutron Polarimetry with Polarized ^{3}He for the NPDGamma Experiment. Dissertation Presented for Doctor of Philosophy Degree, University of Tennessee, Knoxville. May 2014.